

# Nanomechanical Properties of Single-Layer Optical Oxide Thin Films Used for High-Laser-Damage-Threshold Applications

## Introduction

Oxide coatings for optical applications such as high-intensity laser systems must meet stringent specifications of long-lasting optical stability and high laser-damage resistance. Therefore, it is necessary to accurately estimate intrinsic and thermally induced stresses and mechanical properties of these coatings. Silica ( $\text{SiO}_2$ ), hafnia ( $\text{HfO}_2$ ), and alumina ( $\text{Al}_2\text{O}_3$ ) are among the most-important oxide thin-film materials for manufacturing coatings that have high laser-damage thresholds. Examples include high-reflectivity mirrors and polarizers<sup>1</sup> manufactured from multilayer dielectric (MLD) coatings consisting of  $\sim 200$ -nm-thick, alternating low- and high-refractive-index layers ( $\text{SiO}_2$  and  $\text{HfO}_2$ , respectively) coated on glass (fused silica, BK7, etc.) substrates, for a total physical thickness of  $\sim 5$  to  $8 \mu\text{m}$  (Ref. 2). The mechanical properties of the single layers of these oxide thin films with thicknesses equivalent to those used in multilayers are of specific interest to the authors. One important application of these measured values is to study the failure of thin films in a multilayer system composed of alternating layers of silica and hafnia; this application was used in an earlier published work<sup>3</sup> that focused on understanding the fracture mechanics of a defect in optical multilayer thin-film systems when exposed to cleaning procedures. Another application is in the correct measurement and design of mechanical properties (modulus and hardness) of thin-film multilayers. In this application, it is critical to know the accurate properties for individual films that comprise these multilayers.

It is known<sup>4–6</sup> that changing the parameters of the deposition process—namely, oxygen backfill pressure, temperature, and rate of deposition—causes a change in the structural integrity of the thin film, including its porosity and microstructure. This might lead to differences in measured mechanical properties, even under the same test conditions for the same material deposited on an identical substrate. Therefore, when reporting measured mechanical properties of thin films, they should ideally be accompanied by information on deposition parameters, and the reported values should be used only as a reference under those stated deposition conditions.

In this work, nano-indentation on thin, single-layer films are tested and the measured load-displacement curves are used to simultaneously extract the elastic modulus and hardness of these films. These results may be used for more-detailed modeling via effective media theories.

## Experimental Details

Three single-layer thin films— $\text{SiO}_2$ ,  $\text{HfO}_2$ , and  $\text{Al}_2\text{O}_3$ —were grown using electron-beam deposition (EBD), while  $\text{Nb}_2\text{O}_5$  was grown using plasma-ion-assisted electron-beam deposition (PIAD). All depositions were performed in vacuum using the 54-in. coating system shown in Fig. 142.12. Hafnium metal was evaporated from a six-pocket electron-beam gun and oxidized as it condensed at the substrate surface by back-filling the vacuum chamber with oxygen gas to a pressure of  $8.0 \times 10^{-5}$  Torr. Alumina was also deposited from the six-pocket electron-beam source, while silica was deposited from a continuously rotating pan-type electron-beam gun. Niobia was grown by evaporating niobium metal (99.99% pure) as the source material using a single plasma source to energetically assist the electron-beam-deposition process. Using a plasma

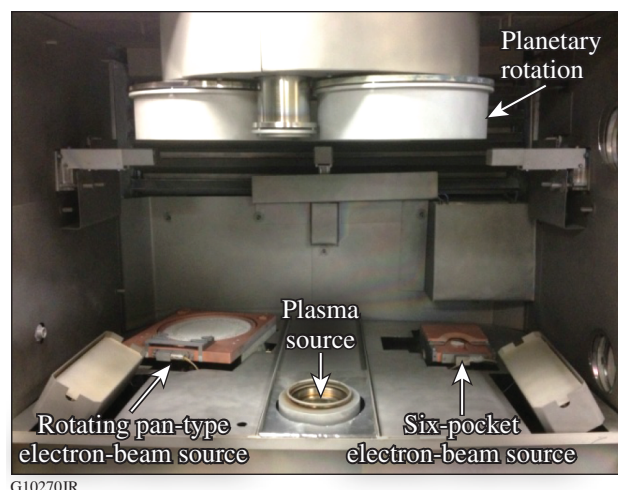


Figure 142.12  
The 54-in. vacuum chamber used to deposit the reported single-layer thin films.

source ensures the complete oxidation of the film, which is otherwise not possible with regular EBD and also allows for a more-energetic process, leading to increased densification of the thin film.<sup>7</sup> The substrate temperature was maintained at 140°C for depositing all films except niobia for which the substrate temperature was 130°C (the authors have established that these were the optimized growth parameters). Deposition was performed on five 25.4-mm-diam × 0.25-mm-thick fused-silica substrates placed in the planetary rotation system for each material deposition. Only one sample of each type of coating was used to perform the nano-indentation experiments. The thicknesses of the deposited single layers along with the process parameters are summarized in Table 142.I. Thicknesses of the films being deposited were monitored and controlled inside the coating chamber using a three-quartz-crystal monitoring setup.

All indentation experiments on these single-layer thin films were performed on the MTS Nano Instruments Nano-indenter XP. The system was fitted with a Berkovich tip, which is a three-sided, pyramidal diamond tip (face angle ~65.03°), and the tip area's function was calibrated by performing nano-indentation on fused silica. This study focused on measuring the hardness and elastic modulus of the single-layer coatings via the Oliver–Pharr method.<sup>8</sup> Typical loads varied from 0.15 to 1.5 mN, and data were obtained for penetration depths amounting up to ~50% of individual film thicknesses. Eight to twelve indents were performed on one sample of each of the single-layer thin films.

The empirical observation,<sup>9</sup> which states that for the reliable measurement of mechanical properties it is necessary that the obtained nano-indentation data have minimal or, if possible, no “substrate effect,” was followed to report near-surface values of elastic modulus and hardness. This implies that the maximum depth of penetration of the indenter tip into the thin film, when making such measurements, should not be more than 10% to 15% of the total film thickness, especially when calculating

the hardness value. Given the significantly small thicknesses (<200 nm) of SiO<sub>2</sub>, HfO<sub>2</sub>, and Al<sub>2</sub>O<sub>3</sub>, various loads ranging from 0.15 to 15 mN were used to generate results for penetration depths varying from 10% to 50% of the total single-layer thickness. On the other hand, Nb<sub>2</sub>O<sub>5</sub> was a slightly thicker film (500 nm) and loads of 0.2 to 15 mN were required to probe 5% to 70% of the total film thickness. Indents were spaced ~100 to 150 μm apart to prevent any overlap.

## Results and Discussions

The cross sections of the films used for testing are shown using scanning electron microscopy (SEM) in Fig. 142.13. It is noteworthy that the interface of the silica film on the silica substrate cannot be seen because of the chemical homogeneity of the film and substrate.

Figure 142.14 shows the load-displacement curves for all measurements, which indicate that there were no anomalies such as “pop-in” events observed in the measurement of the

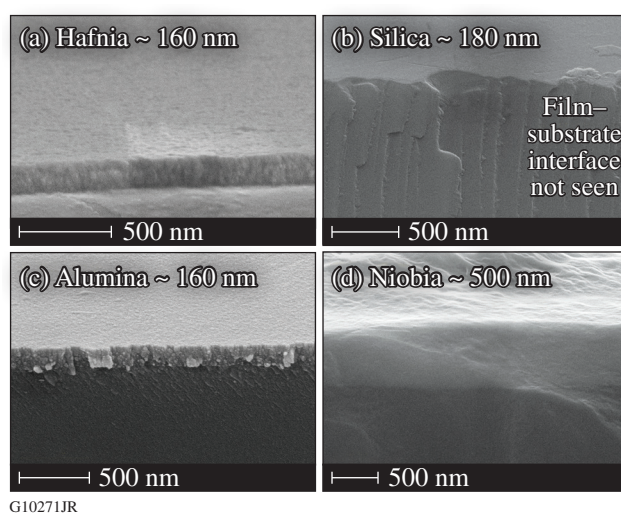
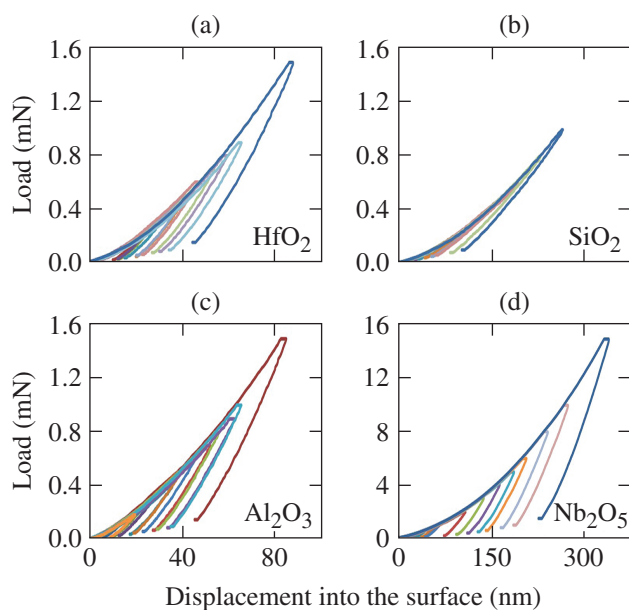


Figure 142.13  
Scanning electron microscope (SEM) images of the thin films used in this study.

Table 142.I: Process parameters for electron-beam deposition (including plasma-assist deposition) of single-layer coatings.

Material	Thickness (nm)	Deposition rate (nm/s); Temperature (°C)	Oxygen backfill pressure (Torr)	Electron-beam voltage (keV)
Hafnia	160	0.15; 140	$8 \times 10^{-5}$	7.5
Silica	180	0.46; 140	not used	6.0
Alumina	160	0.20; 140	$8 \times 10^{-5}$	7.5
Niobia*	500	0.12; 130	not used	6.0

\*55.0 standard cubic centimeters (scm) of O<sub>2</sub> were used as a process gas for reactive deposition above the plasma chamber to increase both the reactivity of the plasma and the oxidation of the film.



G10273JR

Figure 142.14

Load-displacement curves for the four single-layer thin films tested show the different maximum loads and penetration. It should be noted that the abscissae for (a) and (b) are identical to that for (c).

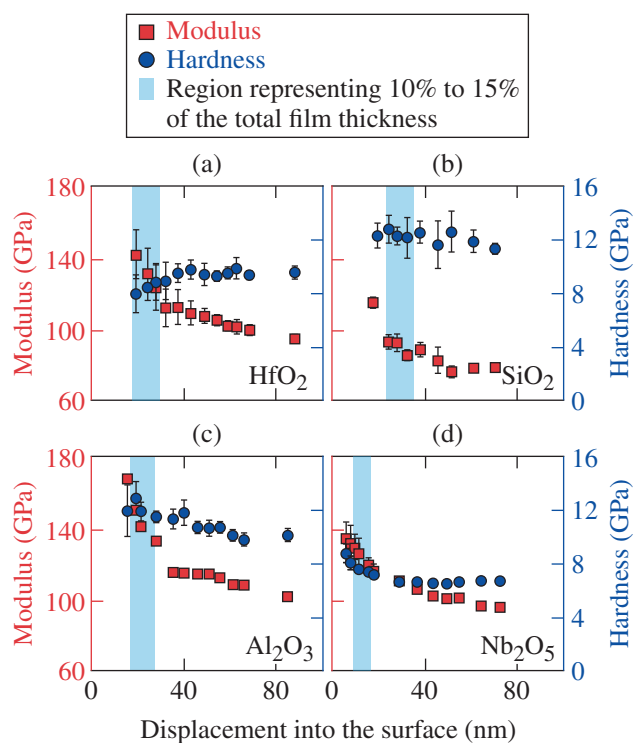
above-reported values and that the tests were, therefore, reliable for reporting the near-surface mechanical properties. Once these data are generated, the elastic modulus and hardness can be reported as a range over the  $\sim 10\%$  to  $15\%$  of the film thickness tested (shown in Fig. 142.15).

Based on the above results, elastic modulus and hardness corresponding to nano-indentation penetration depths of  $\sim 10\%$  to  $15\%$  are reported in Table 142.II. It is noted that these measured values are specifically for the deposition conditions mentioned earlier in the study.

To put these values in perspective and to see how they compare against each other, the extracted mechanical properties of each of the tested films were plotted as the elastic modulus

Table 142.II: Extracted near-surface mechanical properties corresponding to penetration depths of  $\sim 10\%$  to  $15\%$  of the total film thickness.

Single-layer thin film	Elastic modulus (GPa)	Hardness (GPa)
Hafnia	$128 \pm 12$	$8.7 \pm 0.4$
Silica	$93 \pm 5$	$12.3 \pm 0.3$
Alumina	$148 \pm 17$	$12.1 \pm 0.6$
Niobia	$130 \pm 4$	$8.1 \pm 0.5$



G10272JR

Figure 142.15

Measured near-surface values of elastic modulus and hardness for the four single-layer coatings. To generate these data, 8 to 12 indents were performed on one sample of each coating type. The blue band indicates the region of interest and encompasses the values measured for  $\sim 10\%$  to  $15\%$  of the total film thickness for each single layer, respectively. It should be noted that the abscissae for (a) and (b) are identical to those of (c) and (d).

[Fig. 142.16(a)] and hardness [Fig. 142.16(b)]. Alumina has the highest modulus and hardness, which can probably be attributed to the relatively dense film structure without the presence of micro-columnar pores indicated by the fact that these films exhibit tensile stresses while allowing for very slow water-diffusion rates.<sup>10,11</sup> Silica, which is also amorphous, has a high hardness (highest along with alumina) but the lowest modulus among the tested films. Hafnia, deposited using electron-beam technology, is slightly crystalline and has a porous, columnar microstructure<sup>4,12</sup> (shown in the SEM images in Fig. 142.13). It is seen that the measured nano-indentation modulus and hardness of hafnia are very similar to that of niobia. To determine the microstructure of niobia x-ray diffraction (XRD) phase scans, glancing angle scans and texture measurements were conducted on the single-layer thin film. Tests revealed that the film was mostly amorphous, but no conclusions were made about the porosity of the niobia single-layer coating.

Table 142.III compares the measured values and properties of thin films used in the present study to those of films (manu-

factured with the same materials) that are reported in literature, deposited by similar techniques, and used for similar applications such as in optical interference coatings. The measured Young's modulus of the four films used in this study, reported in Fig. 142.17 as "thin film (present study)," is compared to Young's modulus of the same four films from literature<sup>13,14</sup> and is shown as "thin film (literature)." The film values are also compared to bulk values (where data were available). The bulk value was significantly higher than that of any film of the same material (no bulk value of niobia is reported). For films deposited using conventional electron-beam deposition (hafnia, silica, and alumina), the values of modulus reported in the present study were different from the films reported in literature, even though the same growth technique was used, indicating the importance of particulars of the deposition conditions. For hafnia, this difference in modulus can be attributed to

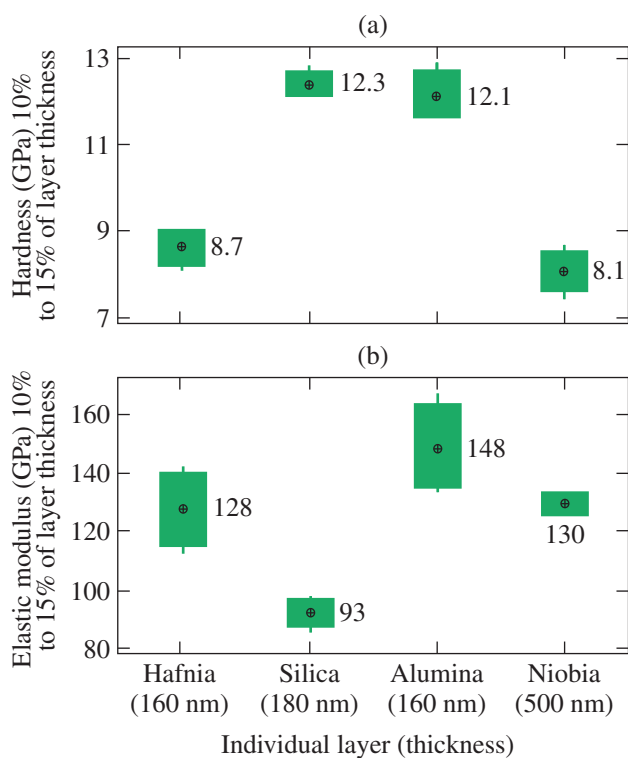
differences in the temperature to which the substrate is heated. Higher substrate temperatures used for hafnia, as reported in the literature,<sup>13</sup> are seen to be associated with films of higher stiffness and lower levels of porosity. Therefore, these films are expected to be much denser than films used in the present study, which have a more-porous microstructure from both the low kinetic energy of the atoms condensing on the substrate and the lower substrate temperatures. It is important to note that this study was not carried out to deposit films whose mechanical properties match with films reported in literature.

The films used in the present study were designed and deposited in a highly controlled way to maximize their laser-damage resistance.<sup>1</sup> The modulus reported in literature for thin-film silica is ~25% lower than what was measured in this study. This result is in contradiction to what one would expect based on the

Table 142.III: Comparison of thin films used in the present study to bulk and film properties reported in the literature.

Sample	Type	Thickness (nm)	Young's modulus (GPa)	Measurement method	Important deposition condition(s); known film properties
Hafnia <sup>13</sup>	Bulk	—	~300*	EMA/EFA-slope ( $d\sigma/dT$ )	—
Hafnia <sup>13</sup>	Thin film (e-beam)	86	~200*	EMA/EFA-slope ( $d\sigma/dT$ )	Substrate temperature 300°C; monoclinic; packing density 0.86 (porosity 0.14)
Hafnia	Thin film (e-beam)	160	128	Present study—nano-indentation	Substrate temperature 140°C; slightly monoclinic with crystallite size ~10 nm; suspected high porosity suggested from SEM images
Silica <sup>13</sup>	Bulk	—	72	EMA/EFA-slope ( $d\sigma/dT$ )	n/a
Silica <sup>13</sup>	Thin film (e-beam)	60	72	EMA/EFA-slope ( $d\sigma/dT$ )	Substrate temperature 300°C; amorphous
Silica	Thin film (e-beam)	180	93	Present study—nano-indentation	Substrate temperature 140°C; amorphous; porous
Alumina <sup>13</sup>	Bulk	—	~400*	EMA/EFA-slope ( $d\sigma/dT$ )	Polycrystalline
Alumina <sup>13</sup>	Thin film (e-beam)	55	~70*	EMA/EFA-slope ( $d\sigma/dT$ )	Amorphous
Alumina	Thin film (e-beam)	160	148	Present study—nano-indentation	Not determined
Niobia	Bulk	—	—	—	—
Niobia <sup>14</sup>	Thin film (PECVD)	550	130	Szymanowski <i>et al.</i> <sup>14</sup> —nano-indentation	100 to 200 sccm of O <sub>2</sub> ; amorphous; H ~ 10 GPa
Niobia	Thin film (PIAD)	500	130	Present study—nano-indentation	55 sccm of O <sub>2</sub> ; amorphous; H ~ 8 GPa; substrate temperature 130°C

\*Indicates that for these materials, biaxial modulus was converted to Young's modulus (using Poisson ratio values<sup>7</sup>) for the purpose of comparison for this study. PEVCD: plasma-enhanced chemical vapor deposition; PIAD: plasma-ion-assisted deposition; EMA/EFA: effective medium approximation/effective field approximation.



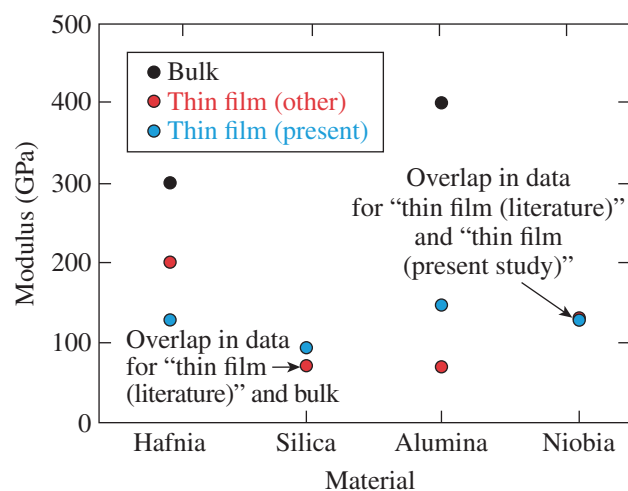
G10274JR

Figure 142.16

(a) Hardness corresponding to penetration depths approximately equal to 10% to 15% of the total film thickness. The data labels on the plots represent the mean of the measured values. (b) Elastic modulus corresponding to penetration depths approximately equal to ~10% to 15% of the total film thickness. The data labels on the plots represent the mean of the measured values.

higher substrate temperatures alone that were used in the study reported in the literature.<sup>13</sup> This clearly indicates that other factors such as deposition rates (shown in Table 142.I for the present study), geometry and size of the coating chamber (54-in. chamber for the present study),<sup>15</sup> and the angle of incidence of coating vapors on the substrate<sup>15</sup> (unknown currently) are also extremely important. It has been shown in literature<sup>16,17</sup> that the thin-film density has a linearly decreasing relationship with the tangent of the incident angle of the evaporant flux, thereby indicating that porosity or void content of the film is increasing. Therefore, the combined effect of these parameters and the way they are controlled will govern the film structure (density and porosity) and, consequently, its mechanical properties.

It is interesting to observe that, even for similar film thicknesses, our data via nano-indentation (present study) yield significantly different elastic modulus values compared to the approach via effective medium approximation. These differences are shown in Fig. 142.17. This suggests that the various coating parameters such as size of the vacuum chamber, depo-



G10275JR

Figure 142.17

Modulus values for the different materials reported in this study in bulk and thin-film forms. No bulk value of niobia is reported.

sition rates used, substrate temperature, as well as deposition angle, might be responsible for this difference. Interestingly, plasma-assist-deposited niobia films (literature and present study) have identical values of modulus (and similar hardness values), even though different amounts of process gas ( $O_2$ ) were used to deposit the respective films. In this case, we surmise that the deposition technique was the dominating factor and changing one of the process parameters had no significant impact on the measured mechanical properties of this thin film.

As an example of this approach, we demonstrate how the properties of single-layer thin film may be used to analyze multilayer dielectric (MLD) thin films used for high-laser-damage-threshold applications. We will select a hafnia-silica multilayer thin-film system, merely as an example, to show how individual thin-film properties (elastic modulus  $E$ ) can be used to predict the shear modulus  $\mu$  and bulk modulus  $B$  for the multilayer thin film using the relations  $\mu = E/2(1 + \nu)$  and  $B = E/3(1 - 2\nu)$ . In this case the volume fractions of hafnia and silica in the multilayer thin-film system are 0.39 and 0.61, respectively. The upper and lower limits on shear modulus and bulk modulus were calculated by the rule of mixtures:

$$(\mu_{\text{MLD}})^{\text{upper}} = \mu_{\text{hafnia}} V_{\text{hafnia}} + \mu_{\text{silica}} V_{\text{silica}},$$

$$(B_{\text{MLD}})^{\text{upper}} = B_{\text{hafnia}} V_{\text{hafnia}} + B_{\text{silica}} V_{\text{silica}},$$

and

$$1/(\mu_{\text{MLD}})^{\text{lower}} = (V_{\text{hafnia}}/\mu_{\text{hafnia}}) + (V_{\text{silica}}/\mu_{\text{silica}}),$$

$$1/(B_{\text{MLD}})^{\text{lower}} = (V_{\text{hafnia}}/B_{\text{hafnia}}) + (V_{\text{silica}}/B_{\text{silica}}),$$

where  $V_{\text{hafnia}}$  and  $V_{\text{silica}}$  are the volume fractions of hafnia and silica. The lower and upper limits on bulk modulus were calculated to be 58.4 GPa and 63.5 GPa, respectively, whereas the limits on shear modulus were found to be 44.5 GPa and 45.2 GPa, respectively. These bounds can now be averaged to estimate the bulk and shear moduli for the multilayer coating. Furthermore, Poisson ratio ( $\nu$ ) and Young's modulus ( $E$ ) for the multilayer coating can also be calculated using the relations  $\nu = (3B - 2\mu)/(6B + 2\mu)$ ,  $E = 2\mu(1 + \nu)$ . In this example, these values work out to be  $\nu_{\text{MLD}} = 0.20$  and  $E_{\text{MLD}} = 108$  GPa. Such material properties can then be used to interpret the underlying fracture mechanics of these multilayer thin-film systems.<sup>3</sup>

### Conclusions

A nano-indentation study was performed on four single-layer thin films used in high-power laser systems to understand their mechanical properties, specifically hardness and Young's modulus. Alumina and silica demonstrate the highest values of hardness and are approximately equal to 12 GPa. The highest value of elastic modulus was also shown by alumina approximately equal to 148 GPa. These measured values were compared to properties reported in the literature for films used in similar applications and grown by identical techniques, but under varying deposition conditions. It is shown that the properties of the film are directly related to not only the deposition techniques, but also the deposition factors, such as substrate temperature, deposition rates, and amount of oxygen used for back-fill and even the geometry and size of the coating chamber. These factors can be controlled to produce thin films for very specific applications such as coatings with high laser-damage thresholds, but changing these parameters can significantly change the film's density and porosity (or the microstructure of the film) and therefore directly affect the hardness and modulus measurements.

It has also been concluded that accurate and reliable measurements of single-layer films are important to understanding the fracture mechanics and failure mechanisms of multilayer thin-film systems manufactured from the same materials. Such properties could also be useful as guidelines in designing multilayers of specified hardness and modulus by controlling the thicknesses and properties of the single-layer thin films.

### ACKNOWLEDGMENT

The authors express their appreciation to the University of Rochester's Laboratory for Laser Energetics (LLE) for continuing support. K. Mehrotra is supported by an LLE Horton Fellowship. The authors also thank Dr. Stephen D. Jacobs for useful discussions and his valuable feedback. This material is

based upon work supported by the Department of Energy National Nuclear Security Administration under Award Number DE-NA0001944, the University of Rochester, and the New York State Energy Research and Development Authority. The support of DOE does not constitute an endorsement by DOE of the views expressed in this article.

### REFERENCES

1. J. B. Oliver, A. L. Rigatti, J. D. Howe, J. Keck, J. Szczepanski, A. W. Schmid, S. Papernov, A. Kozlov, and T. Z. Kosc, in *Laser-Induced Damage in Optical Materials: 2005*, edited by G. J. Exarhos *et al.* (SPIE, Bellingham, WA, 2005), Vol. 5991, Paper 599119.
2. K. Mehrotra, H. P. Howard, S. D. Jacobs, and J. C. Lambropoulos, in *Nanocomposites, Nanostructures and Heterostructures of Correlated Oxide Systems*, edited by T. Endo *et al.*, Mat. Res. Soc. Symp. Proc. Vol. 1454 (Cambridge University Press, Cambridge, England, 2012), pp. 215–220.
3. H. P. H. Liddell, K. Mehrotra, J. C. Lambropoulos, and S. D. Jacobs, *Appl. Opt.* **52**, 7689 (2013).
4. H. Leplan *et al.*, *J. Appl. Phys.* **78**, 962 (1995).
5. R. Thielsch, A. Gatto, and N. Kaiser, *Appl. Opt.* **41**, 3211 (2002).
6. J. E. Klemberg-Sapieha *et al.*, *Appl. Opt.* **43**, 2670 (2004).
7. J. B. Oliver, P. Kupinski, A. L. Rigatti, A. W. Schmid, J. C. Lambropoulos, S. Papernov, A. Kozlov, J. Spaulding, D. Sadowski, Z. R. Chrzan, R. D. Hand, D. R. Gibson, I. Brinkley, and F. Placido, *Appl. Opt.* **50**, C19 (2011).
8. W. C. Oliver and G. M. Pharr, *J. Mater. Res.* **7**, 1564 (1992).
9. J. L. Hay, M. E. O'Herna, and W. C. Olivera, in *Symposium T—Fundamentals of Nanoindentation & Nanotribology*, edited by N. R. Moody *et al.*, Mat. Res. Soc. Symp. Proc. Vol. 522 (Materials Research Society, Warrendale, PA, 1998), p. 27.
10. R. Thielsch *et al.*, *Thin Solid Films* **410**, 86 (2002).
11. J. B. Oliver, P. Kupinski, A. L. Rigatti, A. W. Schmid, J. C. Lambropoulos, S. Papernov, A. Kozlov, C. Smith, and R. D. Hand, *Opt. Express* **20**, 16,596 (2012).
12. J. B. Oliver, S. Papernov, A. W. Schmid, and J. C. Lambropoulos, in *Laser-Induced Damage in Optical Materials: 2008*, edited by G. J. Exarhos *et al.* (SPIE, Bellingham, WA, 2008), Vol. 7132, Paper 71320J.
13. R. Thielsch and N. Kaiser, in *Optical Interference Coatings*, OSA Technical Digest Series (Optical Society of America, Banff, Canada, 2001), Paper ThB6.
14. H. Szymanowski *et al.*, *J. Vac. Sci. Technol. A* **23**, 241 (2005).
15. J. B. Oliver, "Evaporated HfO<sub>2</sub>/SiO<sub>2</sub> Optical Coatings and Modifications for High-Power Laser Applications," Ph.D. thesis, University of Rochester, 2012.
16. Y. D. Fan *et al.*, *Phys. Status Solidi A* **134**, 157 (1992).
17. M. J. Brett, *J. Mater. Sci.* **24**, 623 (1989).